Spin waves in antiferromagnetic FeF_2

1970 J. Phys. C: Solid State Phys. 3 307

(http://iopscience.iop.org/0022-3719/3/2/013)

Spin waves in antiferromagnetic FeF_2†

M. T. HUTCHINGS‡§, B. D. RAINFORD‡¶ and
Clarendon Laboratory, Oxford
H. J. GUGGENHEIM
Bell Telephone Laboratories, Murray Hill, New Jersey, U.S.A.

MS. received 15*th May* 1969

Abstract. Spin-wave dispersion in antiferromagnetic FeF_2 has been investigated by inelastic neutron scattering using a chopper time-of-flight spectrometer. The single mode observed has a relatively flat dispersion curve rising from 53 cm^{-1} at the zone centre to 79 cm^{-1} at the zone boundary. A spin Hamiltonian which includes a single-ion anisotropy constant D ($\mathscr{H}_s^i = -DS_{iz}^2$), three exchange parameters J_l ($\mathscr{H}_{ex}^{12} = J_l \boldsymbol{S}_1 . \boldsymbol{S}_2$) and dipolar interactions has been fitted to the measured energies. We find $D = 6{\cdot}46$ ($+0{\cdot}29$, $-0{\cdot}10$) cm^{-1}, J_1 (coupling neighbouring ions along the c axis) $= -0{\cdot}048$ ($\pm 0{\cdot}060$) cm^{-1}, J_2 (coupling neighbouring ions at the corner and body centre of the cell) $= +3{\cdot}64$ ($\pm 0{\cdot}10$) cm^{-1}, and J_3 (coupling neighbouring ions along the a axis) $= +0{\cdot}194$ ($\pm 0{\cdot}060$) cm^{-1}. Using these parameters we have calculated the density of magnon states and the lineshapes for optical Raman scattering and two-magnon infra-red absorption. The calculated lineshapes are compared with those observed experimentally by other workers.

1. Introduction

Spin-wave dispersion provides the most direct method of determining the interaction constants in an ordered antiferromagnet. (See Keffer 1966 for a comprehensive review of spin waves in magnetic compounds.) The energy of excitation of a spin wave at low temperatures is a simple function of the interaction constants and wave-vector components, and if measurement of the energy is made at a sufficient number of wave vectors the constants may be found uniquely. No theoretical models or approximations need be assumed, apart from the usually well-founded spin-wave theory. This is in contrast to the interpretation of measurements of other bulk properties such as specific heat, susceptibility and magnetization. In this paper we describe the measurement by inelastic neutron scattering of the spin-wave dispersion relations in antiferromagnetic ferrous fluoride, and the use of the experimental results to calculate the density of magnon states and lineshapes for certain optical and infra-red processes.

Ferrous fluoride, FeF_2, orders at 78·4 °K (Stout and Catalano 1955) and has the rutile crystal structure D_{4h}^{14}–$P4/mnm$ (Stout and Reed 1954). The antiferromagnetic structure is the same as that of the other rutiles MnF_2 and CoF_2. The moments are aligned along the c axis and those on the ions at the cell corners are antiparallel to those on the body-centred ions (Erickson 1953). Together with NiF_2, which has a differently ordered spin direction (Moriya 1960 a), and VF_2, which has a spiral spin structure (Hutchings private communication, Lau *et al.* 1969), these compounds form a series which has attracted a great deal of theoretical and experimental interest. This interest has been accentuated in recent years by the discovery of electromagnetic radiation processes involving the spin-wave spectrum.

† A preliminary account of this work was given at the International Congress on Magnetism and Magnetic Materials, Boston, 1967. (See Guggenheim *et al.* 1968.)

‡ On University Attachment to A.E.R.E., Harwell, Didcot, Berks.
§ Now at Brookhaven National Laboratory, Upton, New York, U.S.A.
¶ Now at Atomic Energy Commission, Risø, Roskilde, Denmark.

These are two-magnon infra-red absorption (Halley and Silvera 1965), Raman scattering from magnons (Fleury *et al.* 1966) and the observation of magnon sidebands on optical transitions (Greene *et al.* 1965). A detailed knowledge of the spin-wave dispersion is necessary for the interpretation of the experimental lineshapes of these spectra. All three processes are observed in the rutile antiferromagnets.

FeF_2 is of particular interest also from a theoretical point of view because the ferrous ions are subjected to a large single-ion anisotropy while retaining their spin-only character and interacting with each other through a predominantly isotropic Heisenberg exchange interaction (see Lines 1967, and Tanake *et al.* 1968 for a discussion of this aspect). Previous analyses of data from experiments such as antiferromagnetic resonance, nuclear magnetic resonance, susceptibility and specific heat show that the next-nearest neighbour exchange interaction predominates. However, these analyses all involve some approximation which makes the estimates of the smaller exchange constants somewhat uncertain. The present work was carried out with a view to obtaining more accurate values for all the interactions involved.

In § 2 the experimental techniques are briefly described. In § 3 the theory of the spin-wave dispersion is discussed, and in § 4 the experimental data and their analysis are given. The calculation of the density of magnon states and lineshapes for two-magnon processes is described in § 5. The results are discussed in § 6 and briefly summarized in § 7.

2. Crystal structure and experimental techniques

The sample used for the experiments was a 1 cm × 0·9 cm × 0·7 cm single crystal grown by a modified Bridgman method (Guggenheim 1963) at the Bell Telephone Laboratories. The starting material was synthesized by heat treating 99·999% iron metal powder in a dry hydrogen fluoride atmosphere at 900°C. The crystal had a small mosaic spread, giving Bragg reflections with full width at half maximum intensity of about 10′.

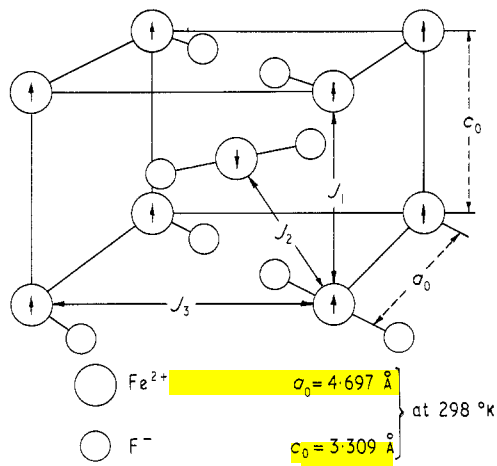

Figure 1. Structure of FeF_2 showing the spin direction and the location of the three nearest types of neighbours.

The rutile crystal structure is shown in figure 1. The cation sites are surrounded by a distorted octahedron of fluorine ions, the point symmetry being D_{2h}. The environment of the corner ions differs from that at the body centre by a rotation of 90° about the *c* axis. Below the Néel temperature the spins align along the *c* axis as shown in figure 1; the magnetic unit cell is the same size as the chemical cell.

The sample, mounted on a goniometer head, was oriented with an ⟨010⟩ axis vertical by x-rays. It was then transferred to a holder which could be mounted in a cryostat at 4·2°K, the sample being immersed in the liquid helium.

The experiments were performed on the twin-rotor chopper spectrometer at the Pluto reactor, A.E.R.E., Harwell. Details of this spectrometer have been described by Dyer and Low (1961).

In the experiments neutrons of wavelength 2·33 Å ($\sim$15 mev $\sim$176°K $\sim$121 cm^{-1}) lost energy to excite a spin wave in the sample. The initial and final neutron energy, $\hbar^2k^2/2m$ and $\hbar^2k'^2/2m$, and momenta, $\hbar\boldsymbol{k}$ and $\hbar\boldsymbol{k}'$, must obey the conservation laws (see e.g. Lomer and Low 1965). So the energy E_q and momentum $\hbar\boldsymbol{q}$ of the spin-wave excitation can be found from the two equations

$$\frac{\hbar^2k^2}{2m} - \frac{\hbar^2k'^2}{2m} = E_q \tag{1}$$

$$\boldsymbol{k} - \boldsymbol{k}' = \boldsymbol{K} = \boldsymbol{\tau} + \boldsymbol{q} \ . \tag{2}$$

Here $\boldsymbol{\tau}$ is reciprocal lattice vector. For the sample orientation used $\boldsymbol{\tau}$ and $\boldsymbol{q}$ lay in the {010} plane. The effects of the finite resolution of the spectrometer were not corrected for explicity, but were included in the error bars on each measured point. Typically, the energy of a given point was determined to 1 cm^{-1}, and the components of $\boldsymbol{q}$ to 0·014 $Å^{-1}$.

3. Theory

3.1. *Single-ion Hamiltonian*

The Fe^{2+} ion has a $3d^6$ configuration and a ^5D ground term. In an octahedral crystal field the orbital degeneracy of the ground term is reduced, and the environment gives rise to a lower triplet and an excited doublet orbital state separated by some 10000 cm^{-1}. However, in orthorhombic D_{2h} symmetry all the orbital degeneracy is removed. The energy of the first excited state above the ground singlet has recently been determined as 1115 cm^{-1} (Stout *et al.* 1968). This is in good agreement with earlier estimates from electron paramagnetic resonance work by Tinkham (1956). The fivefold spin degeneracy of the ground orbital state is removed by spin–orbit coupling and spin–spin interaction within the Fe^{2+} ion. The splitting of these lowest levels may be described by a spin Hamiltonian as introduced by Pryce (1950) and discussed for FeF_2 by Tinkham. This spin Hamiltonian acts on the true spin = 2, and takes the form

$$\mathscr{H}_s^i = -DS_{iz}^2 + E(S_{ix}^2 - S_{iy}^2). \tag{3}$$

The sign of the term in E is reversed for the other site j in the unit cell because of the 90° rotation of its environment. The contributions to D and E from spin–orbit coupling are of order $(\lambda/\Delta)^2$, where $\lambda \sim -63$ cm^{-1} is the spin–orbit coupling constant (Tinkham 1956) and Δ is the energy of the first excited state at 1115 cm^{-1}. There will also be, in principle, fourth-order terms in the spin operators, but these will have coefficients of order $(\lambda/\Delta)^4$ and will be negligible. The splitting of the levels is shown schematically in figure 2. Tinkham (1956) found from electron paramagnetic resonance measurements on Fe^{2+} in ZnF_2 that $D = +7{\cdot}3$ cm^{-1} and $E \sim 0{\cdot}1D$.

3.2. *The crystal Hamiltonian*

We take the main interactions between the ions to be isotropic Heisenberg exchange as there is little orbital content to their moment. The Hamiltonian for the crystal may then be written as

$$\mathscr{H} = \sum_i \mathscr{H}_s^i + \sum_j \mathscr{H}_s^j + \sum_l \sum_{\langle m,\delta_l\rangle} J_l \boldsymbol{S}_m \cdot \boldsymbol{S}_{m+\delta_l} + \mathscr{H}_{dd}. \tag{4}$$

The third term is the exchange term, l is summed over the different types of neighbour, and $\langle m, \delta_l\rangle$ denotes the sum over all pairs of lth neighbour ions m and $m + \delta_l$, each pair of ions being included only once. The first three types of neighbour to a given ion are indicated in figure 1. The fourth term in equation (4) represents the magnetic dipole–dipole interaction. This is a small term which we treat approximately as described below.

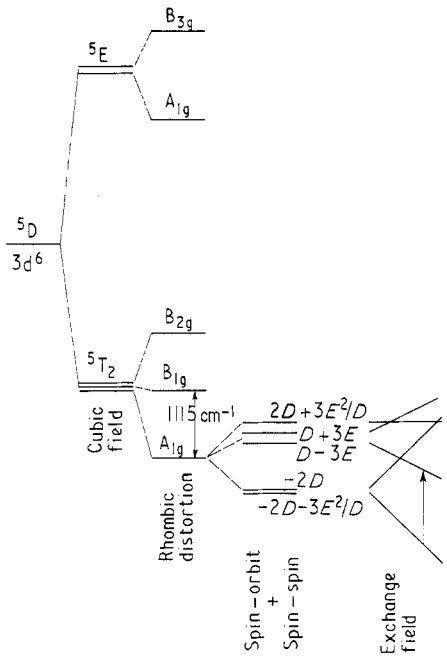

Figure 2. Schematic splitting of free Fe^{2+} ion levels in rutile. The arrow indicates the spin deviation corresponding to the observed magnon mode.

3.3. *Spin-wave energy*

The Hamiltonian is transformed into spin-wave variables in the usual manner (see e.g. Kittel 1964). Care must be taken when expressing the second-degree terms in deviation operators, as has been emphasized by Kanamori and Minatono (1962) and Lines (1967). The spin deviations giving the two degenerate magnon modes observed in our experiments correspond to excitations from the ground $|M_S = -2\rangle$ state to the $|M_S = -1\rangle$ state as shown in figure 2. Modes corresponding to other deviations have very small transition probabilities because E is small. At higher temperatures, $kT \gtrsim 3D$, other modes may be capable of excitation from the higher levels. Diagonalization of the spin-wave Hamiltonian gives the spin-wave energies:

$$E_q = \left(1 + \alpha_q \frac{0{\cdot}065}{2S}\right)(a_q b_q - c_q^2)^{1/2} \tag{6}$$

where

$$a_q = \psi_q^{\mathrm{A}} + S(\gamma'_{\mathrm{a}0} - \gamma'_{\mathrm{p}0} + \gamma'_{\mathrm{p}q}) + 2ES\left(1 - \frac{1}{2S}\right)^{1/2}$$

$$b_q = a_q - 4ES\left(1 - \frac{1}{2S}\right)^{1/2}$$

$$c_q = S\gamma'_{\mathrm{a}q}$$

$$\psi_q^{\mathrm{A}} = \psi_q^{\mathrm{d}} + (2S - 1)D.$$

$\gamma'_{\mathrm{a}q}$ denotes the summation of the Fourier transform of the exchange constant over all spins antiparallel to a reference spin and $\gamma'_{\mathrm{p}q}$ the corresponding sum over all parallel spins. $\gamma'_{\mathrm{a}0}$ and $\gamma'_{\mathrm{p}0}$ are the sums with $q = 0$. Thus, for example,

$$\gamma'_{\mathrm{a}q} = \sum_{\substack{l=\text{anti-}\\ \text{parallel}\\ \text{neighbours}}} \gamma_{lq}$$

where

$$\gamma_{lq} = \sum_{\delta_l} J_l \exp(i\boldsymbol{q} \cdot \boldsymbol{\delta}_l).$$

$\boldsymbol{\delta}_l$ denotes the vector from an ion to its lth neighbour and J_l the corresponding exchange constant.

The term in α_q in equation (6) is the Oguchi factor and ψ_q^d is an effective dipolar anisotropy term. These are discussed below. They are both small terms, affecting the spin-wave energies by about 1–2 cm^{-1}, but were included in an attempt to obtain accurate values for the small exchange constants.

In addition to the terms present in the Hamiltonian equation (5), we might expect a small antisymmetric exchange interaction of the form $\boldsymbol{d}_l \cdot \boldsymbol{S}_{mA}\boldsymbol{S}_{m+\delta_l}$ acting between the next-nearest neighbour ions since these do not have a centre of inversion symmetry between each pair. Moriya (1960 b) estimates such terms to be of order $(\lambda/\Delta)\, J_l$. However, on transforming to spin-wave variables it may be shown that this interaction does not affect the spin-wave energies in first order. We have also omitted all anisotropic exchange interactions. Moriya (1960 b) has estimated the bilinear anisotropic exchange terms to be of order $(\lambda/\Delta)^2 J_l$. Their effect may best be taken into account by adding terms $J_l^{\text{anis}} S_{mz} S_{m+\delta_l' z}$ to the Hamiltonian. However, the largest such interaction, between the next-nearest neighbour ions, will on transforming to spin-wave variables merely give a term which is indistinguishable from that in D. Our final value for D may therefore contain a very small contribution from anisotropic exchange.

In the case in which we include interactions only out to third neighbours, the values for a_q, b_q and c_q in the general expression for the spin-wave energies become

$$\left.\begin{aligned} a_q &= \psi_q^A + S(\gamma_{20} - \gamma_{10} - \gamma_{30} + \gamma_{1q} + \gamma_{3q}) + 2ES\left(1 - \frac{1}{2S}\right)^{1/2} \\ b_q &= a_q - 4ES\left(1 - \frac{1}{2S}\right)^{1/2} \\ c_q &= S\gamma_{2q} \end{aligned}\right\} \quad (7)$$

where

$$\begin{aligned} \gamma_{1q} &= 2J_1 \cos(q_z c) \\ \gamma_{2q} &= 8J_2 \cos(\tfrac{1}{2}q_x a)\cos(\tfrac{1}{2}q_y a)\cos(\tfrac{1}{2}q_z c) \\ \gamma_{3q} &= 2J_3\{\cos(q_x a) + \cos(q_y a)\}. \end{aligned}$$

In table 1 we tabulate the zone centre and zone boundary energies for the special case when $\alpha_q = \psi_q^d = 0$ and $J_2 \gg J_1, J_3$. J_1 and J_3 are seen to remove the degeneracy over the zone boundary and a measurement of the zone boundary energies for different directions

Table 1. Zone centre and zone boundary magnon energies when $\alpha_q = 0$ and $\psi_q^d = \psi_0^d$†

Point		Energy
(0,0,0)	Γ	$\{X(32J_2 + X)\}^{1/2}$
(1,0,0)	X	$X + 16J_2 - 8J_3$
(0,0,1)	Z	$X + 16J_2 - 8J_1$
(1,0,1)	R	$X + 16J_2 - 8J_1 - 8J_3$
(1,1,0)	M	$X + 16J_2 - 16J_3$
(1,1,1)	A	$X + 16J_2 - 8J_1 - 16J_3$

† $X = g\mu_B H_A = (2S - 1)D + \psi_0^d$ = an effective anisotropy energy.
The letters denote the special points shown in the inset of figure 6.

of $\boldsymbol{q}$ enables their values to be determined. The scattering cross section from magnons in rutile structures having this spin-wave dispersion relation has been discussed by Nagai and Yoshimori (1961); their expression shows that the scattering intensity falls of uniformly as q increases.

3.3.1. *Higher order corrections to the spin-wave energy.* The results of retaining only the lowest-order terms in the deviation operators in the Holstein–Primakoff transformation of the Hamiltonian (equation (5)) is the expression for the spin-wave energies given in equation (6) with α_q set equal to zero. This transformation neglects both the kinematical and dynamical interactions (Dyson 1956). Dyson has found the former to be important only near the Néel temperature. The dynamical interactions, which arise from one spin wave scattering from another, correspond to higher-order terms in the expansion in deviation operations of S^+ and S^-. These interactions are expected in an antiferromagnet even at 0°K because of the nature of the ground state. Oguchi (1960) has treated those terms involving products of four spin deviation operators by a perturbation method, and has expressed their effect on the antiferromagnetic spin-wave energy by a multiplicative factor. Although his result is not rigorous, the same method when applied to a ferromagnet does give a result consistent to this order with Dyson's exact expression for the temperature dependence of the spin-wave energies.

In order to calculate the expression for the Oguchi factor appropriate to FeF_2 we must make some approximations. We anticipate our final results and neglect exchange between all ions except the next-nearest neighbours, and we include only the axial single-ion anisotropy. Then, if we define $\epsilon = (2S - 1)\, D/\gamma_{20}S$ and $\gamma_q = \gamma_{2q}/\gamma_{20}$, the factor by which the Holtstein–Primakoff spin-wave energy must be multiplied in order to include the effects of dynamic interactions is

$$1 + \frac{c}{2S}\frac{1 + \epsilon - \gamma_q^2}{(1 + \epsilon)^2 - \gamma_q^2} = 1 + \alpha_q \frac{c}{2S} \tag{8}$$

where

$$\alpha_q = \frac{1 + \epsilon - \gamma_q^2}{(1 + \epsilon)^2 - \gamma_q^2}$$

and

$$c = \frac{2}{N} \sum_{q'} \left[1 - \frac{1 + \epsilon - \gamma_{q'}^2}{\{(1 + \epsilon)^2 - \gamma_{q'}^2\}^{1/2}}\right]. \tag{9}$$

We have calculated c for values of D and J_2 close to our final values and used this number in equations (8) and (6). For $\epsilon = 0{\cdot}344$ we find from numerical integration of equation (9) that $c = 0{\cdot}0647$. The correction factor affects the energies by only about 1%; it has a small dispersion varying by about 50% over the zone. If we put $\epsilon = 0$, the limit of zero anisotropy, the correction factor becomes independent of $\boldsymbol{q}$ and we obtain $c = 0{\cdot}0731$, a result given previously by Anderson (1952) and by Kubo (1952).

We should point out that these factors are frequently omitted in the analysis of antiferromagnetic resonance measurements. Since the antiferromagnetic resonance frequencies are often measured to better than 0·2% the omission would appear to be unjustified.

3.3.2. *Dipolar anisotropy.* Although the dipolar interactions also make only a small contribution to the spin-wave energy, it is relatively straightforward to include them to a fair degree of accuracy, and we have calculated their effect on the spin-wave spectrum with the aid of a computer programme kindly loaned to us by Dr. G. G. Low of A.E.R.E., Harwell. This programme uses the expressions for a simple two-sublattice antiferromagnet with dipolar interactions calculated by Ziman (1952).

We shall not repeat Ziman's rather lengthy formulae here, but only outline the method of treating dipolar effects we have adopted. Ziman's result showed that dipolar interactions may remove the twofold degeneracy of the spin-wave modes, the splitting depending on $\boldsymbol{q}$ and being symmetric about a shifted energy. Low (private communication) has found that the modes remain degenerate along the $\langle 001 \rangle$ direction and over the Brillouin zone boundaries. This behaviour has also been predicted group theoretically by Brinkman and Elliott (1966 a, b). The splitting of the modes, however, is only about 1% of their energy and cannot be detected in our experiments because of the low instrumental resolution. We have therefore used the mean calculated energy. The dipolar contribution to the mean spin-wave energy depends on $\boldsymbol{q}$ in a complicated manner involving lattice sums for each value of $\boldsymbol{q}$, and any iterative fitting procedure would be considerably lengthened if exact calculations were made at every point $\boldsymbol{q}$. We have therefore used an approximate method in which the dipolar contribution to the energy is represented by a simple analytic function determined as follows.

We may define an effective dipolar anisotropy field by the relation

$$\psi^{\mathrm{d}}_{q}\gamma'_{1q} = (E'^{2}_{q} + S^{2}\gamma'^{2}_{aq})^{1/2} - \{(2S-1)D + S(\gamma'_{a0} - \gamma'_{p0} + \gamma'_{pq})\} \tag{10}$$

where E'_q is the mean spin-wave energy calculated with the dipolar interaction included completely in the manner described by Ziman. We have calculated $\psi^{\mathrm{d}}_{\boldsymbol{q}}$ using values for D and J_i which give the best fit to the data with no dipolar interactions. The values obtained for $\psi^{\mathrm{d}}_{\boldsymbol{q}}$ when $\boldsymbol{q}$ lies along the symmetry directions are plotted in figure 3. It is found that

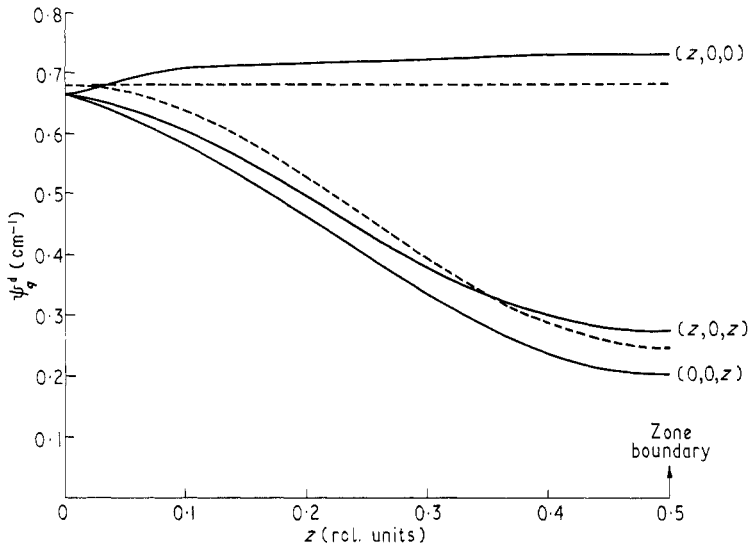

Figure 3. Dispersion of $\psi^{\mathrm{d}}_{\boldsymbol{q}}$. The full lines are calculated from the complete expression (Ziman 1952) using values of D and J_2 close to our final values. The broken curve is calculated from equation (11).

$\psi^{\mathrm{d}}_{\boldsymbol{q}}$ varies mainly with the z component of $\boldsymbol{q}$, a result also found in MnF_2 (Low 1965), and that this variation may be well approximated by a cosine curve. We have therefore taken

$$\psi^{\mathrm{d}}_{\boldsymbol{q}} = 0{\cdot}462 + 0{\cdot}218 \cos\left(\frac{q_z \pi}{q_z^{\max}}\right) \ (\mathrm{cm}^{-1}) \tag{11}$$

as representing the $\boldsymbol{q}$ dependence of the dipolar anisotropy field. The constants in equation (11) were chosen to give the best fit to the complete dispersion shown in figure 3. At $\boldsymbol{q} = 0$, $\psi^{\mathrm{d}}_{0} = 0{\cdot}68\ \mathrm{cm}^{-1}$. E_0 is thus affected by about 1·3%, and E_{ZB} by about 0·3%.

4. Experimental results

Spin waves were observed about reciprocal lattice points $\tau = (001)$ and (100) in the manner described in § 2. Settings were used so that some values of $\boldsymbol{q}$ lay along the symmetry directions. Counting times of between 6 and 24 h were necessary for low $\boldsymbol{q}$ and zone boundary spin waves respectively. In all, excitations at some 261 points in reciprocal space were observed and their distribution is shown in figure 4. The pattern of points sampled arises from the use of two banks of four counters each. The fact that most of these points lie at random positions in the Brillouin zone, typical of chopper data, is no handicap in cases such as the present, when a closed theoretical expression for E_q is available. The energies of only those spin waves having wave vectors close to a $\langle 100 \rangle$ or $\langle 001 \rangle$ direction are shown in figure 5.

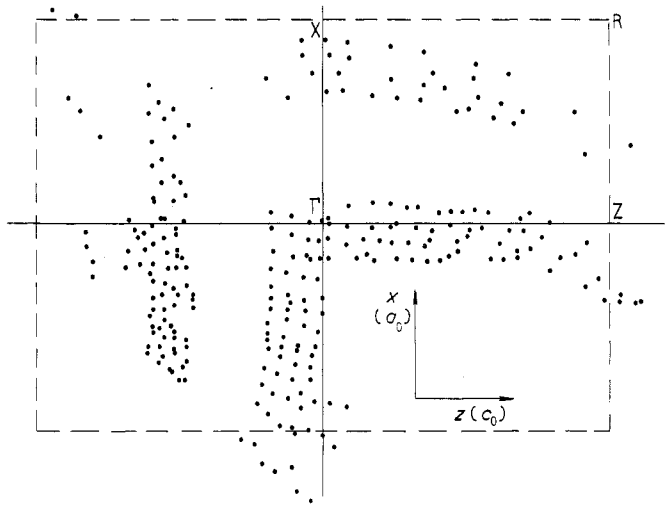

Figure 4. Section of Brillouin zone showing values of $\boldsymbol{q}$ at which the magnon energy was found experimentally.

The expression given in equation (6) was fitted to the experimental points using a generalized least-squares computer routine written by M. J. D. Powell of A.E.R.E., Harwell (Powell 1965). The routine minimized a weighted sum of the squares of the difference between experimental and calculated spin-wave energies. Full details of the procedure are given by Rainford (1969). As the rhombic anisotropy term E affects the spin-wave energies only as a factor of order $(1 - E^2/E_q^2)$, and $E^2/E_q^2 \lesssim 10^{-3}$, we may safely neglect E when fitting to the experimental data, and this constant cannot be determined from our results.

A large number of fits were made to the experimental data under different conditions and some of the results are given in table 2, rows B(i)–(iii). The effects of pinning the antiferromagnetic resonance frequency E_0 at the value of 52·7 ($\pm$0·2) cm^{-1} (Ohlmann and Tinkham 1961), and of omitting the small Oguchi term and dispersion of the dipolar term, were tested. The results can be seen from table 2. Also given in table 2 is the fit obtained if one includes only the next-nearest neighbour exchange constant and omits the Oguchi and dipolar terms. In the final fit E_0 was fixed at 52·7 cm^{-1}; in this way we utilize the higher accuracy of the antiferromagnetic resonance result and counteract the effect of the instrumental resolution which tends to make the measured neutron energy near $q = 0$ too high.

The final values giving the best fit of the full relation, equation (6), to the data are listed in the top row of table 2. The errors quoted are estimates based on the results of all the trial fits made as well as on the experimental data errors. In the best fit only 49 of the 261 calculated points lay outside the experimental error bars, and nearly all of these fell within twice these errors. The values verify that D and J_2 are the predominant interaction parameters. J_1 is very small and ferromagnetic, although the error limits cannot rule out a

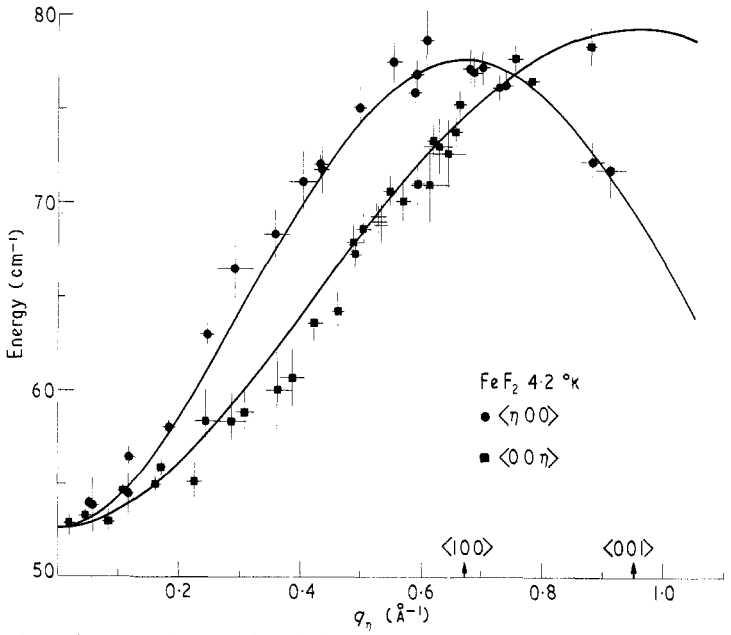

Figure 5. The points are the energies of those spin waves observed which lie close to two symmetry directions. The error bars represent estimates of the probable uncertainty in the measurements. The full curves are calculated from equations (6) and (7) using parameters giving the best fit to the data *throughout* the zone.

Table 2. Values obtained for parameters (in cm^{-1})in the spin Hamiltonian for FeF_2 by fitting to the neutron data with different approximations

	D	J_1	J_2	J_3
A	$6{\cdot}46 \begin{matrix}+0{\cdot}29 \\ -0{\cdot}10\end{matrix}$	$-0{\cdot}048 \pm 0{\cdot}060$	$3{\cdot}64 \pm 0{\cdot}10$	$0{\cdot}194 \pm 0{\cdot}060$
B(i)	6·69	−0·074	3·57	0·159
B(ii)	6·34	0·012	3·73	0·209
B(iii)	6·81	—	3·61	—
C	6·94	—	3·51	—

A, best fit to full Hamiltonian equation (5) including dipolar interaction dispersion and the full Oguchi factor. Final result.
B(i), best fit including dipolar interaction and Oguchi factor in full but not fixing E_0 at 52·7 cm^{-1}.
B(ii), fit obtained omitting Oguchi factor (i.e. $\alpha_q = 0$), and omitting the dispersion of the dipolar interaction. E_0 fixed at 52·7 cm^{-1}.
B(iii), fit obtained with $\alpha_q = \psi_q^d = J_1 = J_3 = 0$. E_0 is fixed at 52·7 cm^{-1} and D will include the dipolar interaction.
C, values obtained with $\alpha_q = \psi_q^d = J_1 = J_3 = 0$. J_2 and D are calculated from $E_0 = 52{\cdot}7\ cm^{-1}$, and $E_{ZB} = 77{\cdot}1\ cm^{-1}$. D will include the dipolar interaction.

zero or antiferromagnetic value, while J_3 is larger and antiferromagnetic. These parameters will be discussed in § 6. Using them we calculate the zone boundary energies to be $E_{001}(Z) = 79{\cdot}2\ cm^{-1}$, $E_{100}(X) = 77{\cdot}7\ cm^{-1}$, $E_{101}(R) = 77{\cdot}7\ cm^{-1}$, $E_{110}(M) = 76{\cdot}1\ cm^{-1}$ and $E_{111}(A) = 76{\cdot}1\ cm^{-1}$, with errors of $\pm 2\ cm^{-1}$. The labels are the symmetry points designated in figure 6. It is sometimes useful to represent the dispersion by a formula which reproduces the approximate spin-wave energies in a simple manner. The values of J_2 and D in row C of table 2 are calculated from E_0 and a weighted average of the above zone boundary energies at the five special points.

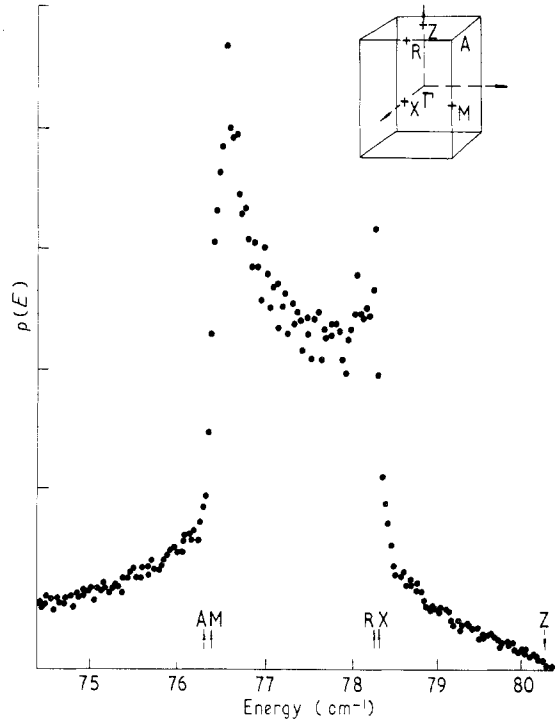

Figure 6. The density of one-magnon states calculated from the final parameters. The corresponding two-magnon density of states is found by doubling the abscissa values. The inset shows the special points in the Brillouin zone.

Mention should be made that the effects of the more distant neighbours J_4 and J_6 were investigated. It was found that these only marginally improved the fit and their fitted values were very small. Their inclusion affected only the value of D. The experimental data are not accurate enough to justify assigning a non-zero value to these parameters. It should be noted that the exchange constants determined can in principle include contributions from other interactions having the same effect in an $\{010\}$ plane. Thus J_3 could contain a small contribution from J_5, but again such contributions are expected to be small.

In none of the experiments were any phonon excitations observed. This is not surprising as the settings used were only designed to pick up the magnon excitations and only low values of $\boldsymbol{K}$ were used. The B_{1g} phonon has an energy of 73 cm^{-1} at the zone centre (Porto *et al.* 1967) compared with the magnon energy of 52·7 cm^{-1}. In CoF_2 (Martel *et al.* 1968) and MgF_2 (Kahn *et al.* 1969) this branch rises as $\boldsymbol{q}$ increases towards the zone boundary and it is therefore unlikely that it crosses the magnon dispersion curves. The acoustic phonon branches, on the other hand, almost certainly cross the magnon curve but they were not detected in our experiments.†

5. Density of spin-wave states and lineshapes

In this section we shall present the results of calculations of the density of magnon states in FeF_2 and of the lineshapes for Raman scattering and two-magnon absorption. These calculations use the final interaction parameters given in the previous section.

5.1. *Density of magnon states*

The density of states may be determined by a summation of magnon wave vector $\boldsymbol{q}$ over the Brillouin zone:

$$\rho(\omega) = \sum_{q} \delta(\omega - \omega_q).$$

† Recent measurements by one of us (B.D.R.) and J. C. G. Honmann using a triple-axis spectrometer have shown the presence of an interaction between the magnon mode and an acoustic phonon band.

The result of a summation with $\boldsymbol{q}$ stepping over 729000 points in the complete zone is given in figure 6. The labels refer to the special points in the zone illustrated in the inset. Van Hove singularities occur at the points R and X and near the points A and M. The peak in $\rho(\omega)$ occurs at a slightly higher energy than that corresponding to the latter two points because the dispersion has a maximum energy at a wave vector below that at the zone boundary.

5.2. *Magnon effects in electromagnetic radiation spectra*

In the last three or four years a large amount of work has been carried out on photon absorption and scattering processes involving spin waves in antiferromagnets. First-order processes, such as antiferromagnetic resonance and one-magnon Raman scattering, give only a measure of the magnon energy at $q = 0$. However, there are three second-order processes which involve magnons of all wave vectors. These give rise to second-order Raman scattering, two-magnon absorption and magnon sidebands. Loudon (1968) and Fleury and Loudon (1968) have reviewed in some detail recent theoretical and experimental work on these processes, and they emphasize the usefulness of symmetry arguments in discussing the selection rules and the form of the coupling Hamiltonian involved. We shall quote briefly their results here.

All three second-order processes are found to give rise to spectra which are electric dipolar in character. This indicates that the photon must couple to a pair of magnetic ions which undergo simultaneous transitions. Three mechanisms have been proposed to account for the interactions between such a pair of ions in intermediate excited states, and each may play a role in certain circumstances. However, as is emphasized by Loudon, the results of group theory hold whatever the microscopic origin of the interaction.

Quite generally group theory indicates that for certain polarizations only excitations at certain symmetry points are emphasized in the spectra, the intensity from magnons at other points being zero. Furthermore, if it is assumed that the photon couples to ion pairs which are connected by an intermediate-state interaction which only acts between nearest neighbour ions on opposite sublattices, the form of the coupling Hamiltonian may be written down and used to find the transition probability. The lineshapes for Raman scattering and two-magnon absorption, the two cases to which we apply our results, are thus found to be given by expressions which are essentially a sum over the two-magnon density of states weighted by a trigonometrical function which depends on the process and polarization of the scattered radiation. These expressions are given below. We have used them to calculate the lineshapes in order to see how well the optical and infra-red measurements tie in with our neutron results.

Raman scattering:
$$I(\omega_2) = \sum_q (u_q^2 + v_q^2)^2 \, W^2 \delta(\omega_1 - \omega_2 - 2\omega_q) \tag{14a}$$

Two-magnon absorption:
$$I(\omega) = \sum_q W^2 \, \delta(\omega - 2\omega_q). \tag{14b}$$

Here u_q and v_q are coefficients occurring in the diagonalization of the spin-wave Hamiltonian and give the amount of excitation on each sublattice (see eg. Fleury and Loudon 1968). In our calculations we used approximate values for u_q and v_q determined when $J_1 = J_3 = 0$. As the factor $u_q^2 + v_q^2$ varies only slowly in the region of q in which the density of two-magnon states is peaked this introduces no error. The final values of the parameters in the full Hamiltonian were used to calculate ω_q, a total of 216000 points in the zone being included in the summation. W is a trigonometrical function given in table 3; for different polarizations it emphasizes the special points in the zone indicated in the table. These points have energies which differ by multiples of the small exchange constants J_1 and J_3, as may be seen from table 1.

The calculated lineshapes are given in figures 7 and 8 where they are compared with the experimental data of Fleury (private communication), Fleury and Loudon (1968) and

Table 3. Trigonometrical weighting factors W occurring in equations (14)†

Polarization		Point emphasized	Weighting factor
Raman	xx, yy, zz	Γ	$\cos(\frac{1}{2}q_x a)\cos(\frac{1}{2}q_y a)\cos(\frac{1}{2}q_z c)$
	xy, yx	M	$\sin(\frac{1}{2}q_x a)\sin(\frac{1}{2}q_y a)\cos(\frac{1}{2}q_z c)$
	xz, zx	R	$\sin(\frac{1}{2}q_x a)\cos(\frac{1}{2}q_y a)\sin(\frac{1}{2}q_z c)$
Two-magnon absorption	$\boldsymbol{E}\parallel c$ axis	A	$\sin(\frac{1}{2}q_x a)\sin(\frac{1}{2}q_y a)\sin(\frac{1}{2}q_z c)$
	$\boldsymbol{E}\perp c$ axis	X	$\cos(\frac{1}{2}q_x a)\sin(\frac{1}{2}q_y a)\cos(\frac{1}{2}q_z c)$

† The letters refer to the special points indicated in figure 6.

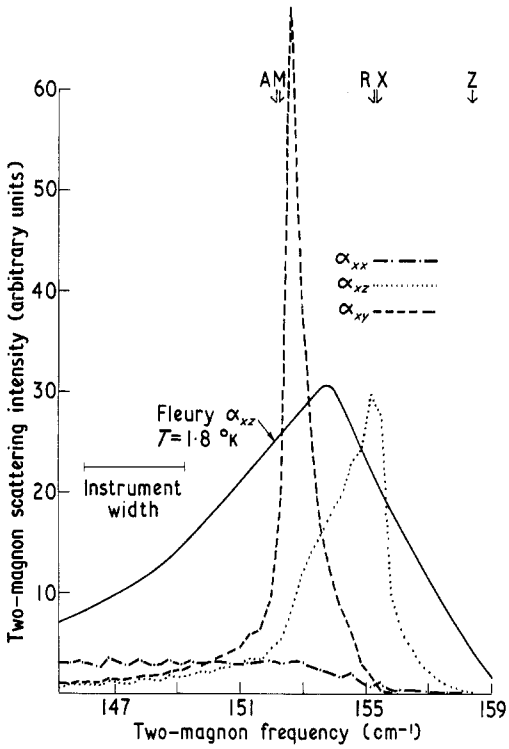

Figure 7. Raman scattering lineshapes calculated from equation (14*a*) for three polarizations. The vertical scale is arbitrary. The full curve is the experimental result of Fleury (private communication).

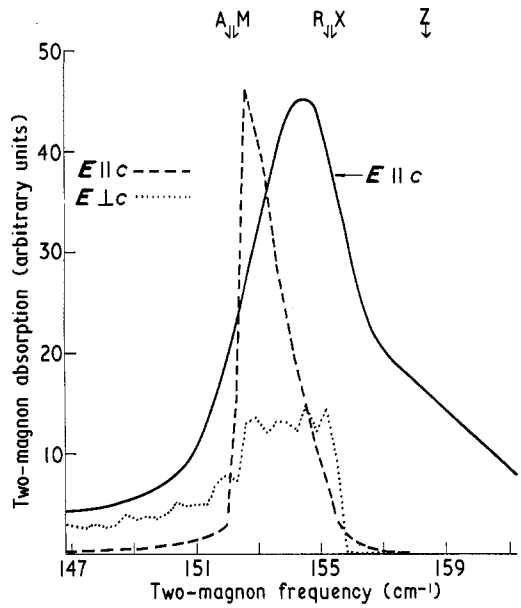

Figure 8. Two-magnon lineshapes calculated from equation (14*b*) for two polarizations. The vertical scale is arbitrary. The full curve is the experimental result of Allen (Richards 1967).

Allen (see Richards 1967). The peaks in the experimental Raman scattering for xz polarization and in the two-magnon absorption for $\boldsymbol{E}\parallel c$ are in very reasonable agreement with those calculated. However, the calculated lineshapes are narrower than observed; they would be broadened somewhat if the effects of the resolution of the optical instruments were included.

In MnF_2, which was the first case in which a detailed comparison between calculated and experimental two-magnon and Raman lineshapes was made (Allen *et al.* 1966, Fleury *et al.* 1967), it is thought that the interaction mechanism coupling the ions in their intermediate states is predominantly exchange. Although the lineshapes could be reproduced quite well assuming only next-nearest neighbour excited state exchange interactions, a more detailed fit to the data had to invoke an extended range of exchange interaction.

More recently, however, it has been suggested that as the photon creates two excitations in close proximity the effect of the interactions between the excitations must be included (Elliott *et al.* 1968). In the case of $RbMnF_3$, an antiferromagnet with one very dominant ground state exchange interaction, an excellent interpretation of the Raman spectrum is obtained from Green function theory by the inclusion of magnon–magnon interactions without the need for long-range exchange between the excited states (Thorpe and Elliott 1969, Elliott and Thorpe 1969). In this straightforward case, the Raman line is shifted through the interactions by about J cm^{-1} from the peak in the density of states, that is by the amount predicted from a simple Ising model of the interactions. In a general case, however, where there is ground state exchange between more than one type of neighbour one cannot see the effects of magnon–magnon interaction in a simple manner. In fact both real and imaginary parts of the crystal Green function must be calculated using the particular values of the exchange constants for the case in point. This Green function is only now available for MnF_2, and very recently Thorpe (private communication) has found that the two-magnon lineshapes in MnF_2 may also be accounted for fully by the inclusion of magnon–magnon interaction. However, the shift of the lines no longer bears a simple relationship to the density of states, and may be less than that expected on the Ising model.

In order to estimate the effects of magnon–magnon interaction on the lineshapes in FeF_2, for which there is no complete crystal Green function available, Thorpe (private communication) has approximated the Green function by use of a simple model (see Elliott and Thorpe 1969) in which the only parameters in the spin Hamiltonian are J_2 and D, α_q and ψ_q^d in equation (6) being set equal to zero. The values used for these two parameters are those given in the bottom row of table 2. Thorpe's results are shown in figures 9 and 10. The shift from the non-interacting theory peak, which would occur at

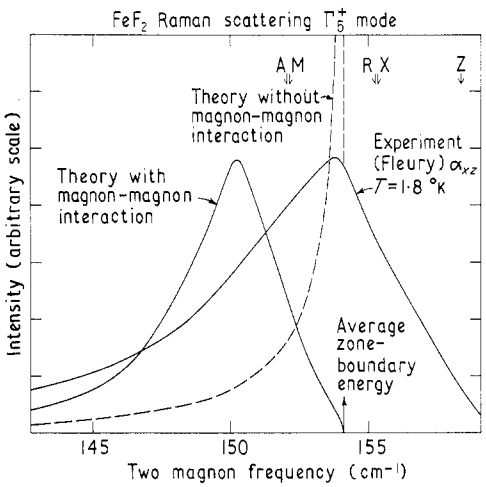

Figure 9. Comparison of the experimental Raman lineshape with that calculated, including magnon–magnon interaction but assuming a simplified ground state Hamiltonian fitted to the average zone boundary energy (Thorpe, private communication).

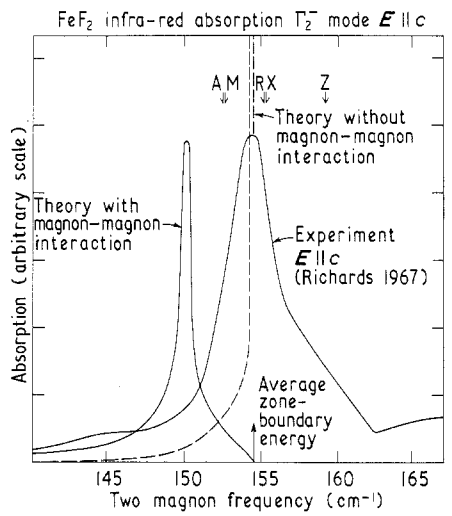

Figure 10. Comparison of the experimental two-magnon absorption lineshape with that calculated by Thorpe (private communication).

154·2 cm^{-1} on his model, is evident. However, the agreement in position of the line is destroyed. The calculated lineshape for Raman scattering is much closer to that observed experimentally than for the non-interacting theory, but that for the two-magnon scattering is still too narrow. Convolution with the instrumental resolution would again improve the agreement.

Clearly a complete calculation, without approximations, should give a result between those shown in figures 7–10, which in a sense are due to two rather extreme theories. In view of the fact that the various effects all shift the calculated peak over a relatively very small range of energy, and both neutron and optical data have some associated experimental error, the general agreement of the calculated peaks is quite satisfactory. A more detailed understanding must await complete calculations.

6. Discussion

In this section we shall compare the parameters derived in § 4 with those found from measurements of other properties of FeF_2.

The anisotropy of FeF_2 was first analysed by Kanamori and Minatono (1962) who used the antiferromagnetic resonance and the zero-temperature perpendicular susceptibility to obtain a value for D of 6·5 cm^{-1}, close to the present value. More recently Fleury and Loudon (1968) have used both the one- and two-magnon Raman scattering data to obtain estimates of D and J_2. They assumed only a next-nearest neighbour ground state interaction, J_2, and neglected magnon interactions to obtain the values given in the fourth row of table 4.

Table 4. Values of interaction parameters in FeF_2 (in cm^{-1}) defined as in equation (5)†

	D	J_1	J_2	J_3
Present work (A of table 2)	$6{\cdot}46 \pm {}^{0{\cdot}29}_{0{\cdot}10}$	$-0{\cdot}048 \pm 0{\cdot}060$	$3{\cdot}64 \pm 0{\cdot}10$	$0{\cdot}194 \pm 0{\cdot}060$
Lines 1967	$6{\cdot}27 \pm 0{\cdot}30$	$0{\cdot}38 \pm 1{\cdot}0$	$3{\cdot}85 \pm 0{\cdot}20$	—
Kanamori and Minatono 1962	6·5			
Fleury and Loudon 1968	6·7		3·50	
Tinkham (Fe^{2+} in ZnF_2) 1956	$7{\cdot}3 \pm 0{\cdot}7$			

† Allowance has been made for dipolar interactions.

By far the most thorough previous treatment is that of Lines (1967) in which an analysis was made using several items of experimental data. These were the antiferromagnetic resonance frequency and its splitting in a magnetic field, the temperature variation of the sublattice magnetization as measured by nuclear magnetic resonance, and the low and high temperature susceptibility measured parallel and perpendicular to the c axis. The data was fitted to only three constants, D, J_1 and J_2, and the result is given in the second row of table 4. The values of D and J_2 fall within the experimental errors of our more accurate results, and, although J_1 is somewhat larger than our value, the accuracy is low. It is interesting to note that if J_3 had been included in Lines' analysis it would occur in the molecular field expressions with J_1 in the form $(z_1J_1 + z_3J_3)$, where z_i is the number of ith neighbours. From our results we obtain a value of $+0{\cdot}68$ cm^{-1} for this summation compared with Lines' value of $\pm 0{\cdot}76$ cm^{-1}. If the positive sign is taken for Lines' value of J_1 the two results are seen to be quite consistent. Finally, for comparison, we give in the bottom row of table 4 the electron spin resonance results of Tinkham (1956) on Fe^{2+} in ZnF_2, a diamagnetic compound isostructural to FeF_2. We see that D is somewhat larger in ZnF_2 than in the concentrated compound. It should be noted that in all the above work the Oguchi factor was not included in the analysis of the antiferromagnetic resonance, but dipolar interactions were included in the form ψ_0^{d}.

It is interesting to compare the values obtained for the interaction constants in FeF_2 with those found in other rutile compounds, and in table 5 we list the values available at the present time. In most cases J_2 dominates and J_1 and J_3 are relatively small. In VF_2, however, J_1 must be *greater* than J_2 by a factor greater than 10 in order to account for the

Table 5. Comparison of effective anisotropy and exchange constants (in cm $^{-1}$)in rutile fluorides

	T_N(°K)	Magnetic structure	Spin, or effective spin⁺	Effective anisotropy energy ($g\mu_B H_A$)	J_1	J_2	J_3
VF_2 (i)	7·0	a	$\frac{3}{2}$	—	$J_1 > 10J_2$		—
MnF_2 (ii)	66·5	b	$\frac{5}{2}$	0·74	−0·44	2·45	0·06
FeF_2 (iii)	78·4	b	2	20·1	−0·05	3·64	0·19
CoF_2 (iv)	37·7	b	$\frac{3}{2}^+$	—	−0·83	4·54	—
NiF_2 (v)	73·2	c	1	—	−0·22	13·87	0·79

Structures: a, spiral along *c* axis, spins in *ab* plane.
b, type 1 body-centred tetragonal, spins parallel to *c* axis.
c, type 1 body-centred tetragonal, spins canted in *ab* plane.

(i) Hutchings (private communication).
(ii) Okazaki *et al.* (1964) Nikotin *et al.* (1969).
(iii) This work.
(iv) Values quoted by Belorizky *et al.* (1969) as private communication from R. A. Cowley. These are obtained using the theory of Lines (1965) and neutron scattering results of Martel *et al.* (1968).
(v) Hutchings *et al.* (to be published).

spiral magnetic structure (Hutchings, private communication). The series should provide a rigorous test for theories of superexchange.

7. Summary

Spin-wave dispersion in an {010} plane of FeF_2 has been investigated by inelastic neutron scattering. A spin Hamiltonian has been fitted to the observed magnon energies at points throughout the Brillouin zone, and the result verifies that the predominant interactions are a large single-ion anisotropy and an exchange between the next-nearest neighbour ions. Dipolar interactions and the effect of higher-order terms in the spin-wave variables have been included in the analysis in order to obtain accurate values for the relatively much smaller exchange constants between first and third neighbour ions. The values of the interaction parameters determined in this manner have been compared with the results of analyses of other experimental data with which there is general agreement.

From the measured parameters the density of magnon states and the lineshapes for Raman scattering and two-magnon absorption have been calculated. The experimental lines agree quite well in energy with the results of simple calculations in which magnon–magnon interaction is neglected. The inclusion of magnon–magnon interaction by Thorpe using a model of next-nearest neighbour exchange only, improves the lineshape agreement, but cannot account rigorously for the exact peak positions. The relatively small discrepancies in position may be due to a number of causes between which we cannot distinguish.

Acknowledgments

This work was carried out using facilities provided by A.E.R.E., Harwell, and was supported in part by the Science Research Council. One of us (B.D.R.) wishes to acknowledge the receipt of a Science Research Council Research Studentship. We are very grateful to G. G. Low for discussions on dipolar anisotropy and for the use of his computer programme to calculate this effect. We would like to thank M. F. Thorpe for several useful discussions on two-magnon lineshapes and for allowing us to present the results of his calculations of magnon–magnon interaction effects. We are also grateful to P. A. Fleury for sending us his results prior to publication. Helpful discussions have also been held with M. F. Collins, R. J. Elliott, R. Loudon, R. D. Lowde, J. Owen and C. G. Windsor. G. A. Briggs, A. C. Harris, N. S. Clark and A. T. Slater gave invaluable technical assistance.

References

ALLEN, S. J., LOUDON, R., and RICHARDS, P. L., 1966, *Phys. Rev. Lett.*, **16**, 463–6.

ANDERSON, P. W., 1952, *Phys. Rev.*, **86**, 694–701.

BELORIZKY, E., NG, S. C., and PHILLIPS, T. G., 1969, *Phys. Rev.*, **181**, 467–77.

BRINKMAN, W., and ELLIOTT, R. J., 1966 a, *J. Appl. Phys.*, **37**, 1457–9.

—— 1966 b, *Proc. R. Soc.* A, **294**, 343–58.

DYER, R. F., and LOW, G. G., 1961, *Inelastic Scattering of Neutrons in Liquids and Solids* (Vienna: International Atomic Energy Agency), pp. 179–94.

DYSON, F. J., 1956, *Phys. Rev.*, **102**, 1217–30, 1230–44.

ELLIOTT, R. J., and THORPE, M. F., 1969, *J. Phys.* C: *Solid St. Phys.*, **2**, 1630–43.

ELLIOTT, R. J., THORPE, M. F., IMBUSCH, G. F., LOUDON, R., and PARKINSON, J. B., 1968, *Phys. Rev. Lett.*, **21**, 147–50.

ERICKSON, R. A., 1953, *Phys. Rev.*, **90**, 779–85.

FLEURY, P. A., and LOUDON, R., 1968, *Phys. Rev.*, **166**, 514–30.

FLEURY, P. A., PORTO, S. P., CHEESMAN, L. E., and GUGGENHEIM, H. J., 1966, *Phys. Rev. Lett.*, **17**, 84–7.

FLEURY, P. A., PORTO, S. P., and LOUDON, R., 1967, *Phys. Rev. Lett.* **18**, 658–62.

GREENE, R. L., SELL, D. D., YEN, W. M., SCHAWLOW, A. L., and WHITE, R. M., 1965, *Phys. Rev. Lett.*, **15**, 656–9.

GUGGENHEIM, H. J., 1963, *J. Appl. Phys.*, **34**, 2482–5.

GUGGENHEIM, H. J., HUTCHINGS, M. T., and RAINFORD, B. D., 1968, *J. Appl. Phys.*, **39**, 1120–1.

HALLEY, J. W., and SILVERA, I., 1965, *Phys. Rev. Lett.*, **15**, 654–6.

KAHN, R., TROTIN, J. P., CRIBIER, D., and BENOIT, C., 1969, *Proc. Copenhagen IAEA Conf. on Inelastic Scattering of Neutrons*, 1968 (Vienna: International Atomic Energy Agency), pp. 289–93.

KANAMORI, J., and MINATONO, M., 1962, *J. Phys. Soc. Japan*, **17**, 1759–66.

KEFFER, F., 1966, *Handb Phys.*, Ed. S. Flügge (Berlin: Springer-Verlag), Vol. XVIII/2, pp. 1–273.

KITTEL, C., 1964, *Quantum Theory of Solids* (New York, London: Wiley), pp. 49–73.

KUBO, R., 1952, *Phys. Rev.*, **87**, 568–80.

LAU, H. Y., STOUT, J. W., KOEHLER, W. C., and CHILD, H. R., 1969, *J. Appl. Phys.*, **40**, 1136.

LINES, M. E., 1965, *Phys. Rev.*, **137**, A982–93.

—— 1967, *Phys. Rev.*, **156**, 543–51.

LOMER, M., and LOW, G. G., 1965, *Thermal Neutron Scattering*, Ed. P. A. Egelstaff, (London, New York: Academic Press), pp. 38–45.

LOUDON, R., 1968, *Adv. Phys.*, **17**, 243–80.

LOW, G. G., 1965, *Inelastic Scattering of Neutrons in Liquids and Solids* (Vienna: International Atomic Energy Agency), pp. 453–60.

MARTEL, P., COWLEY, R. A., and STEVENSON, R. W. H., 1968, *Can. J. Phys.*, **46**, 1355–70.

MORIYA, T., 1960 a, *Phys. Rev.*, **117**, 635–47.

—— 1960 b, *Phys. Rev.*, **120**, 91–98.

NAGAI, O., and YOSHIMORI, A., 1961, *Prog. Theor. Phys.*, **25**, 595–602.

NIKOTIN, O., LINGÅRD, P. A., and DIETRICH, O. W., 1969, *J. Phys.* C: *Solid St. Phys.*, **2**, 1168–73.

OGUCHI, T., 1960, *Phys. Rev.*, **117**, 117–23.

OHLMANN, R. C., and TINKHAM, M., 1961, *Phys. Rev.*, **123**, 425–34.

OKAZAKI, A., TUBERFIELD, K. C., and STEVENSON, R. W. H., 1964, *Phys. Lett.* **8**, 9–11.

PORTO, S. P. S., FLEURY, P. A., and DAMEN, T. C., 1967, *Phys. Rev.*, **154**, 522–6.

POWELL, M. J. D., 1965, *Computer J.*, **7**, 303–7.

PRYCE, M. H. L., 1950, *Proc. Phys. Soc.* A, **63**, 25–9.

RAINFORD, B. D., 1969, *D. Phil. Thesis*, Oxford University.

RICHARDS, P. L., 1967, *J. Appl. Phys.*, **38**, 1500–4.

STOUT, J. W., and CATALANO, E., 1955, *J. Chem. Phys.*, **23**, 2013–22.

STOUT, J. W., and REED, S. A., 1954, *J. Am. Chem. Soc.*, **76**, 5279–81.

STOUT, J. W., STEINFELD, M. I., and YUZURI, M., 1968, *J. Appl. Phys.*, **39**, 1141–2.

TANAKE, T., LIBELO, L., and KLIGMAN, R., 1968, *Phys. Rev.*, **171**, 531–40.

THORPE, M. F., and ELLIOTT, R. J., 1969, *Proc. Int. Conf. on Light Scattering*, New York, 1968 (New York: Springer-Verlag), pp. 199–206.

TINKHAM, M., 1956, *Proc. R. Soc.* A, **236**, 535–48, 549–63.

ZIMAN, J. M., 1952, *Proc. Phys. Soc.* A, **65**, 540–7.